THE JOURNAL OF PHYSICAL CHEMISTRY C

Article

pubs.acs.org/JPCC

High Surface Reactivity and Water Adsorption on $NiFe_2O_4$ (111) Surfaces

Priyank V. Kumar,[†] Michael P. Short,[‡] Sidney Yip,[‡] Bilge Yildiz,*[,‡] and Jeffrey C. Grossman*[,†]

[†]Department of Materials Science and Engineering, and [‡]Department of Nuclear Science and Engineering, Massachusetts Institute of Technology, Cambridge, Massachusetts 02139, United States

Supporting Information

ABSTRACT: Transition metal-doped ferrites are attractive candidates for a wide range of applications including catalysis and electronic and magnetic devices. Although their bulk characteristics are well-understood, very little is known about their surface properties at the molecular level. Here, we demonstrate high reactivity of $NiFe_2O_4$ (111) surfaces, a Ni-doped ferrite, by elucidating the surface structure and water adsorption mechanism using density functional theory with on-site correction for Couloumb interaction (DFT + U). The surface reactivity of $NiFe_2O_4$ (111) surfaces (with 0.25 ML Fe_{tet1} and 0.5 ML $Fe_{oct2-tet1}$ terminations) is shown to be significantly higher in comparison with the undoped Fe_3O_4 (111) surfaces. Dissociation of water is found to be highly favorable with an adsorption energy of −1.11 eV on the 0.25 ML Fe_{tet1} terminated surface and −2.30 eV on the 0.5 ML $Fe_{oct2-tet1}$ terminated surface. In addition, we computed a low activation barrier of 0.18 eV for single water molecule dissociation on the 0.25 ML Fe_{tet1} termination, while the corresponding dissociation reaction on the 0.5 ML $Fe_{oct2-tet1}$ termination proceeded without a barrier. The reactivity of $NiFe_2O_4$ surfaces toward water is understood based on strong interactions between the adsorbing OH radical molecular orbitals and the d orbitals of the surface Fe atom. In particular, the new bonding orbitals created due to the interaction of the OH 3σ orbital and the Fe d states are pushed deeper down the energy axis resulting in a greater energy gain and higher water adsorption strength in the case of 0.5 ML $Fe_{oct2-tet1}$ termination. Furthermore, transition-metal surface resonances (TMSR) are found to be good descriptors of the surface reactivity in the two ferrites investigated and is a useful measure to design ferrite-based catalytic systems. These findings have strong implications toward the use of $NiFe_2O_4$ as an effective metal-doped ferrite catalyst in a typical industrial process such as the water-gas shift (WGS) reaction and are of significance in fuel materials durability in nuclear reactors where ferrites are known to trap boron resulting in failure of the reactors.

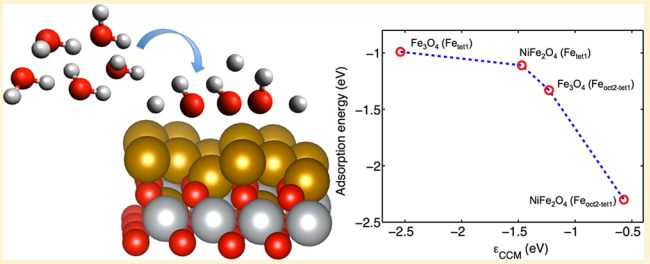

INTRODUCTION

Metal oxide surfaces offer great potential for a wide variety of catalytic applications.[1] Transition-metal ferrites such as magnetite (Fe_3O_4) and metal-doped magnetites are one such oxide family which find use as catalysts in important industrial reactions such as the water-gas shift (WGS) reaction,[2,3] in which CO reacts with water vapor to form CO_2 and H_2. Ferrite thin films also play a crucial role in magnetic recording, microwave magnetic devices, and magneto-optical applications among many others.[4] The reason for such versatile electronic and magnetic properties in ferrites is primarily attributed to the unique distribution of cations in octahedral and tetrahedral sites.[4] Fe_3O_4 and $NiFe_2O_4$ are two such promising candidates for catalysis,[3,5] multiferroic heterostructures, and spintronics devices.[6] In addition, Fe_3O_4 and $NiFe_2O_4$ are one of the major components of the corrosion deposits on nuclear fuel rods.[7,8] Their reactive surfaces are known to trap boron and cause failure of nuclear reactors.[9,10]

Understanding the surface structure and reactivity of Fe_3O_4 and $NiFe_2O_4$ is crucial for designing efficient ferrite-based catalysts for important industrial reactions, such as the WGS reaction ($CO + H_2O = H_2 + CO_2$). In particular, the process of water adsorption and dissociation on ferrite surfaces is identified to be one of the rate-limiting steps in the WGS reaction.[11] Experiments by Costa et al.[12] have shown higher catalytic activity of $NiFe_2O_4$ over the commercial catalyst, Fe_2O_3−Cr_2O_3, used in the low temperature WGS reaction. Recent experiments[3,5] have also reported high yields of CO conversion on Ni-doped Fe_3O_4 catalyst. However, clear insights on the surface structure of $NiFe_2O_4$ and its connection to the surface reactivity is still lacking.

To address some of these issues, adsorption of water on undoped Fe_3O_4 (111) surfaces have been studied via DFT earlier.[11,13] STM experiments on Fe_3O_4 (111) surfaces have recently confirmed the dissociated water molecule configuration (OH* + H*) to be the most favorable state.[14] In the case of $NiFe_2O_4$, DFT calculations[6,15,16] have helped understand structural, electronic, and magnetic properties of bulk

Received: September 22, 2012
Revised: February 10, 2013
Published: March 7, 2013

   dx.doi.org/10.1021/jp309434a | J. Phys. Chem. C 2013, 117, 5678−5683

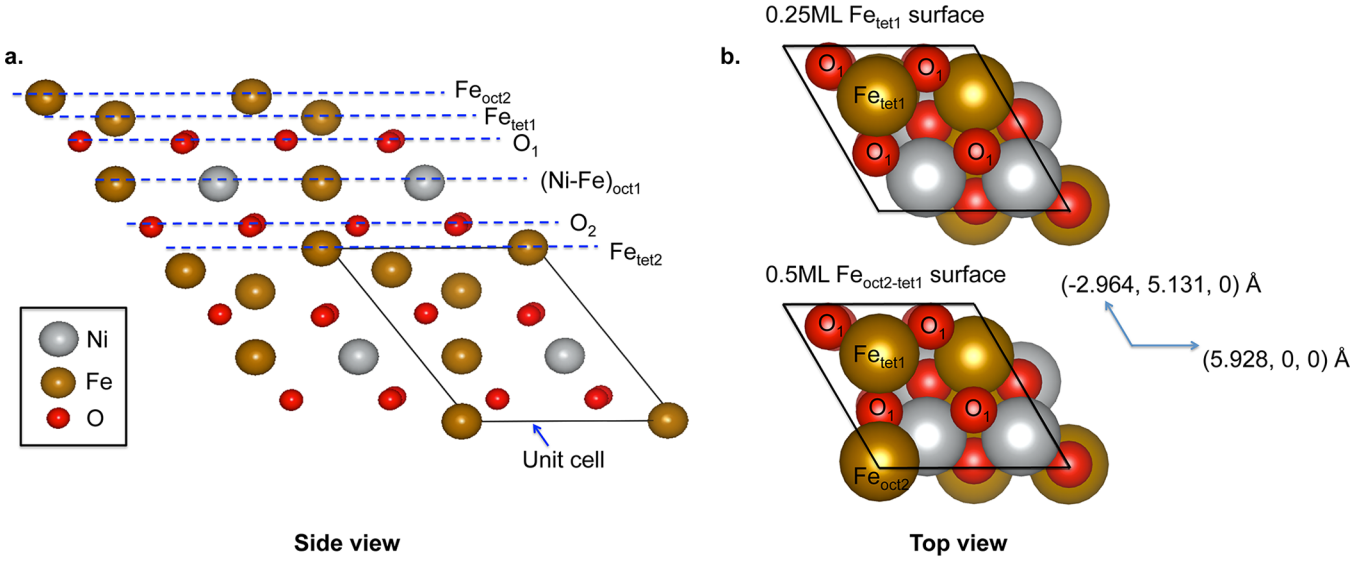

Figure 1. (a) Side view of the $NiFe_2O_4$ (111) structure showing various terminations and the unit cell. (b) Top views of the 0.25 ML Fe_{tet1} and the 0.5 ML $Fe_{oct2-tet1}$ terminations showing the surface Fe atoms and the oxygen plane (O_1) underneath. The surface unit cell vectors are also given.

$NiFe_2O_4$. However, the surface structure of $NiFe_2O_4$ surfaces and its impact on the catalytic activity and strength of water adsorption have been largely unexplored which is an important step toward understanding doped ferrite systems. To fill this gap, we shed light on the mechanism of water adsorption and dissociation on $NiFe_2O_4$ and compare the surface reactivity of $NiFe_2O_4$ and undoped Fe_3O_4.

Nickel ferrite crystallizes in an inverse spinel structure. The unit cell consists of oxygen atoms at FCC positions. An equal number of Ni^{2+} and Fe^{2+} ions occupy the octahedral positions, whereas the tetrahedral positions are occupied by the rest of the Fe^{3+} ions. The ground state is ferrimagnetic with the atoms in octahedral and tetrahedral sites maintaining opposite spins.[15] Hydrothermal synthesis of $NiFe_2O_4$ nanoparticles shows faceted octahedra enclosed by (111) planes.[17] In another experiment, SEM and TEM studies reveal nanocrystalline ferrite particles with well-defined polygonal growth patterns with (111) faceting.[18] Thus it is reasonable to conclude that the predominant growth facet of $NiFe_2O_4$ is the (111) orientation, analogous to the case of Fe_3O_4.[11]

Here, we study the surface structure, energetics and kinetics of water adsorption and dissociation reactions on $NiFe_2O_4$ (111) surfaces using the DFT + U approach. We report higher surface reactivity of $NiFe_2O_4$ (111) over Fe_3O_4 (111) surfaces, and build a descriptor for assessing and tuning the surface reactivity of ferrite-based systems using the concerted-coupling model (CCM) based on surface resonances (SRs).[19]

COMPUTATIONAL METHOD

All DFT calculations have been performed using the Vienna Ab initio Simulation Package (VASP).[20] The projector augmented wave (PAW) method[21] is used to describe the core electrons. Explicitly, the valence electronic configurations of $4s^13d^9$, $4s^13d^7$, and $2s^22p^4$ are used to describe Ni, Fe and O atoms in all simulations. A spin-polarized GGA formalism in the form of Perdew–Wang functional (PW91)[22] is used for exchange-correlation. To account for the strong electron correlations in $NiFe_2O_4$, we employ the DFT + U scheme of Dudarev et al.[23] with a $U - J$ value of 3 eV for both the transition metal cations, a value previously used and tested for consistency of the electronic and magnetic structure with experiments.[6] In order to compare our results with the undoped Fe_3O_4 ferrite system, we used a $U - J$ value of 3.8 eV for Fe atoms in Fe_3O_4, whose surface structure and computational details have been previously described.[11,13]

The $NiFe_2O_4$ (111) surface is constructed using the slab model. As shown in Figure 1a, six ideal bulk terminations are possible upon cleaving along the (111) orientation. The configurations we consider include the 0.25 ML Fe_{tet1} termination and the 0.5 ML $Fe_{oct2-tet1}$ termination as they result in the least number of broken bonds at the surface (Figure 1b). In addition, we consider the oxygen-rich O_1 termination, which is expected to become favorable at higher oxygen partial pressures. The lower half of our slab is constructed with a complete six layer unit, as shown in Figure 1a, which is treated as the bulk and is kept fixed during relaxation. On top of this bulk unit, we relax the surface layer to simulate the 0.25 ML Fe_{tet1}, 0.5 ML $Fe_{oct2-tet1}$ and O_1 terminations. A vacuum space of 12 Å is maintained in all the simulations. A Monkhorst-Pack $3 \times 3 \times 1$ grid is used for k-point sampling.[24] A Gaussian smearing approach with $\sigma = 0.05$ eV has been used and dipole corrections along the slab normal are considered. The plane-wave energy cutoff is fixed at 600 eV. The ions are relaxed until the Hellman-Feynman forces on each relaxed ion are smaller than 0.03 eV/atom. The nudged elastic band (NEB) method, as implemented in VASP, is used for calculating the activation barriers of the dissociation reactions.

The adsorption energy of the water molecule is calculated using the expression

$$E_{ads} = E_{(slab+molecule)} - E_{slab} - E_{molecule} \quad (1)$$

where E_{slab} represents the energy of a clean slab, $E_{molecule}$ represents the energy of the adsorbate in the gas phase, and $E_{(slab+molecule)}$ represents the total energy after adsorption. A negative adsorption energy indicates exothermicity and favorable adsorption.

RESULTS AND DISCUSSION

Pristine $NiFe_2O_4$ (111) Surfaces. The stability of three terminations considered is assessed via ab initio surface

dx.doi.org/10.1021/jp309434a | J. Phys. Chem. C 2013, 117, 5678–5683

thermodynamics. The calculated surface energy diagram is shown in Figure 2. The procedure for obtaining such phase

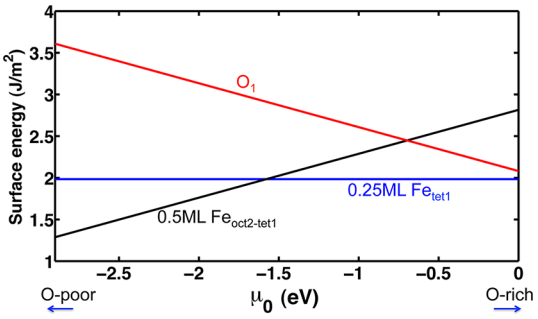

Figure 2. Calculated surface energy as a function of oxygen chemical potential for the three surface terminations studied. The plot is obtained between the O-poor and O-rich limits, with $1/2E^{gas}_{O_2}$ as zero reference.

diagrams is detailed elsewhere.[25] The chemical potentials of bulk $NiFe_2O_4$, bulk Fe, bulk Ni and O_2 molecule have been approximated using the calculated internal energies at 0 K. The standard gibbs free energy of formation of $NiFe_2O_4$ (ΔG^o_f) is obtained from the literature.[26] The allowed range of oxygen potential is between the O-poor and O-rich conditions; the O-poor limit ($1/4\Delta G^o_f$) marks the region where the ferrite dissociates into corresponding metal crystals and O_2 gas, and the O-rich limit (zero reference) is set as the chemical potential of oxygen in the O_2 molecule ($1/2E^{gas}_{O_2}$). Our results indicate that both the 0.25 ML Fe_{tet1} and the 0.5 ML $Fe_{oct2-tet1}$ surface terminations could be stabilized depending on the oxygen partial pressure, the former being stable at higher partial pressures while the latter at lower partial pressures. Hence, we assess the surface activity of these two surfaces.

Adsorption of H_2O on $NiFe_2O_4$ (111) Surfaces: Energetics and Kinetics. The most stable configurations for water adsorption on the 0.25 ML Fe_{tet1} and 0.5 ML $Fe_{oct2-tet1}$ Fe_3O_4 (111) surfaces have been reported.[11,13] A single water molecule is shown to dissociate while a hydronium-ion-like configuration ($H_3O^+-OH^-$) is found to be stable upon adsorption of two water molecules. We tried multiple initial configurations and found similar adsorption structures to be favorable on $NiFe_2O_4$ (111) surfaces for one and two water molecules, as shown in Figure 3. The adsorption energy values for the four configurations are listed in Table 1

Table 1. Comparison of Adsorption Energies of Water Molecules (in eV) on $NiFe_2O_4$ and Fe_3O_4 (111) Surfaces

	$NiFe_2O_4$	Fe_3O_4
Fe_{tet1} ($1H_2O$)	−1.11	−0.99[a]
Fe_{tet1} ($2H_2O$)	−0.95	−0.87[a]
$Fe_{oct2-tet1}$ ($1H_2O$)	−2.30	−1.33[b]
$Fe_{oct2-tet1}$ ($2H_2O$)	−1.51	−1.09[b]

[a]Reference 13. [b]Reference 11.

and are compared to the values obtained with Fe_3O_4 as the adsorbent. Clearly, the exothermicity computed is higher on both the terminations of the $NiFe_2O_4$ (111) surface, and hence we conclude that water adsorption on $NiFe_2O_4$ surfaces is more favorable than on Fe_3O_4 surfaces.

The kinetics of water dissociation reactions on $NiFe_2O_4$ (111) surfaces is also of enormous significance in catalysis and nuclear energy systems. We find that single water molecule dissociation on the $NiFe_2O_4$ (111) 0.25 ML Fe_{tet1} termination has an activation barrier of 0.18 eV and the dissociated state is more stable than the molecular state by 0.24 eV (Figure 4). In the case of 0.5 ML $Fe_{oct2-tet1}$ termination, we found that molecular adsorption is unstable, i.e., although we started our DFT relaxation from a molecularly adsorbed configuration of water molecule, we ended up with a dissociated water molecule state after the relaxation, suggesting that the dissociation reaction is barrierless or has a low activation barrier (<0.1 eV). Turning our attention to the case of adsorption of two water molecules, it has been reported that dissociation becomes

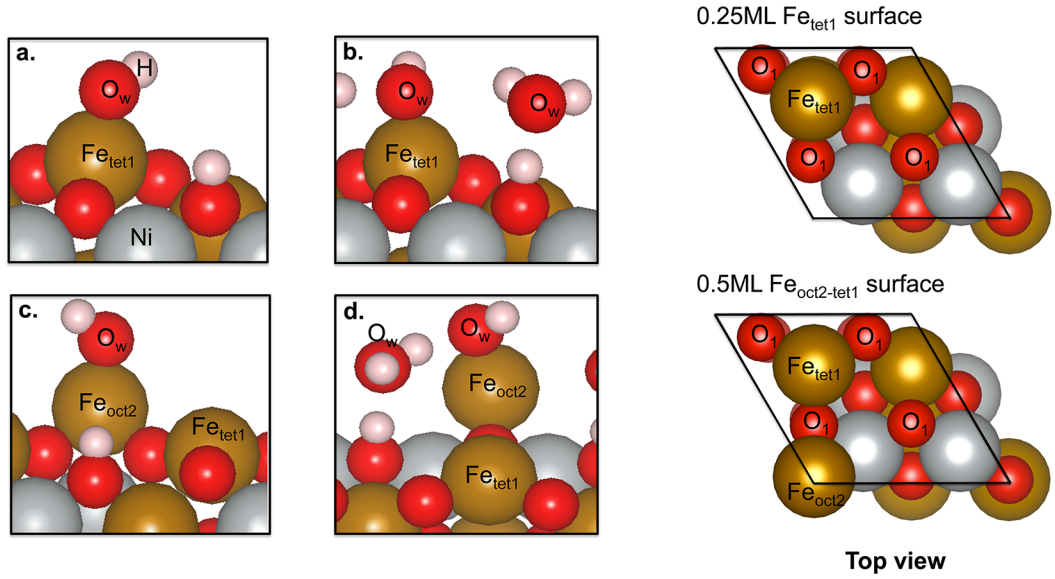

Figure 3. Most stable adsorption configurations of one and two water molecules on $NiFe_2O_4$ (111) surfaces: (a) 0.25 ML Fe_{tet1} − $1H_2O$, (b) 0.25 ML Fe_{tet1} − $2H_2O$, (c) 0.5 ML $Fe_{oct2-tet1}$ − $1H_2O$, and (d) 0.5 ML $Fe_{oct2-tet1}$ − $2H_2O$. The O atoms of the adsorbing water molecules are marked as O_w along with the surface Fe atoms for clarity. The corresponding unit cell top views for the pristine case are also shown.

dx.doi.org/10.1021/jp309434a | J. Phys. Chem. C 2013, 117, 5678−5683

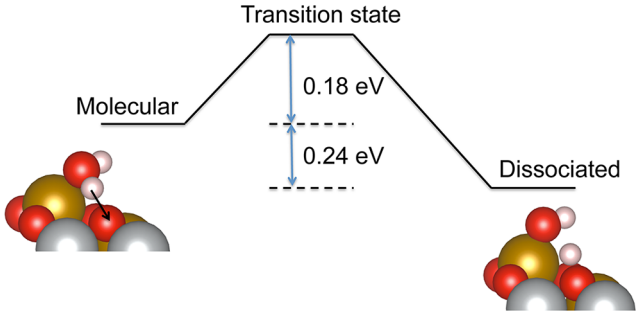

Figure 4. Reaction pathway of a single water molecule dissociation on $NiFe_2O_4$ 0.25 ML Fe_{tet1} terminated surface showing an activation barrier of 0.18 eV. The corresponding reaction on the 0.5 ML $Fe_{oct2-tet1}$ termination was nearly barrierless.

nearly barrierless on Fe_3O_4 (111) surfaces owing to favorable interaction between the two molecules.[11] We observed similar barrierless dissociation, as with the single water molecule dissociation on the 0.5 ML $Fe_{oct2-tet1}$ termination, on the adsorption of two water molecules on $NiFe_2O_4$ (111) surfaces.

Our thermodynamic and kinetic studies of water adsorption on $NiFe_2O_4$ surfaces indicate high reactivity to water and have direct implications in catalytic reactions. For example, one of the crucial steps in the WGS reaction is the dissociation of water molecule into OH* and H* radicals on the surface. A larger exothermicity and lower activation barriers of the surface reactions studied here indicate favorable water molecule dissociation on the surface making available the necessary OH^- ions for CO oxidation in the WGS reaction. Although surface reactions of water at the molecular level have been unexplored on the $NiFe_2O_4$ surfaces, recent STM experiments support favorable dissociation of water on Fe_3O_4 surfaces, which we also confirmed at the DFT level of theory. Furthermore, macro-scale experiments by Costa et al.[12] have shown higher CO conversion efficiencies of $NiFe_2O_4$ over the commercial catalyst, $Fe_2O_3-Cr_2O_3$, used in the low temperature WGS reaction. Taken together, these results suggest that employment of $NiFe_2O_4$ as a catalyst could possibly be favorable in terms of achieving higher reaction rates and better CO conversion efficiencies and could allow for lower process temperatures.

In the context of nuclear reactors, the high surface reactivity of $NiFe_2O_4$ provides preliminary insight into the capability of $NiFe_2O_4$ in trapping boron-rich species such as the boric acid on the surface. Thus, $NiFe_2O_4$ could play a significant role in the corrosion of nuclear fuel rods by facilitating faster boron incorporation reactions when compared to other corrosion deposits including Fe_3O_4, NiO and ZrO_2 which show significant activation barriers for such reactions.[10] We found these results to be in tune with experiments that have shown high adsorption strength of boric acid on $NiFe_2O_4$ and Fe_3O_4 surfaces compared to NiO and ZrO_2,[7] although boric acid reactions must be studied in greater detail on $NiFe_2O_4$ surfaces to quantify the relevant adsorption processes.

Bonding Mechanism Based on the Surface Electronic Structure. In order to connect the surface reactivity and water adsorption strength to the surface electronic structure, we compute the surface Fe projected density of states (PDOS) and the states of the adsorbing OH radical for the 0.25 ML Fe_{tet1} and 0.5 ML $Fe_{oct2-tet1}$ surface terminations. Since the most stable adsorption configuration is a dissociated water molecule state, the bonding mechanism can be understood from the interaction of the molecular orbitals of the OH radical with the d orbitals of the surface Fe atom. Such an interaction leads to the disappearance of pristine O and Fe states which indicates bonding, and the creation of new bonding/antibonding states.[27]

Figure 5 compares the OH states and Fe d-orbital states of the bare surface and dissociated water molecule cases on the two surface terminations. In both these cases, the PDOS shows a strong interaction between the d states of the surface Fe atom and the OH states resulting in the formation of new, broad hybridized states deeper down the energy axis indicating favorable adsorption in both these cases. To understand why the adsorption strength is higher on the 0.5 ML $Fe_{oct2-tet1}$ surface compared to the 0.25 ML Fe_{tet1} surface, we take a closer look at the interaction between the OH 3σ states and the Fe d states within the energy range −5 to −8 eV. If we compare the

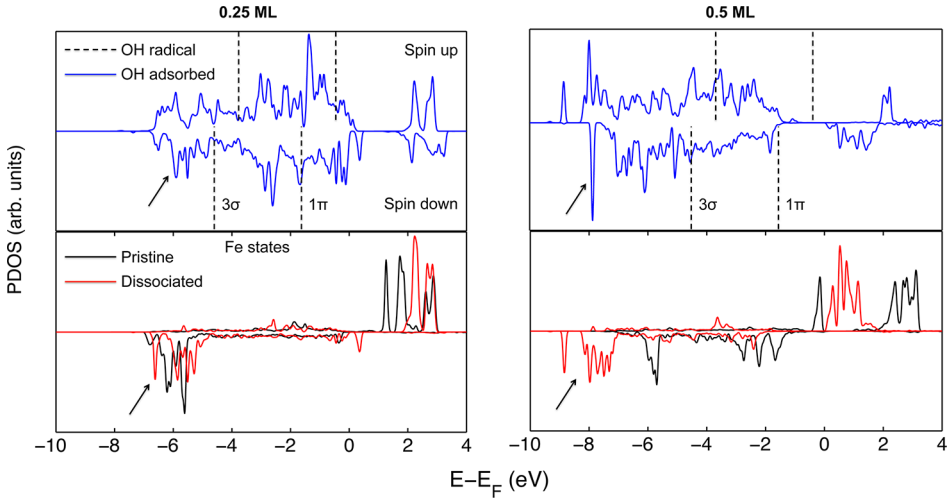

Figure 5. Plot comparing the PDOS of the oxygen atom attached to the adsorbed OH and the molecular orbitals (3σ and 1π) of an isolated OH radical (top panel). Similar comparison of the d states of the surface Fe atom for $NiFe_2O_4$ (111) structures in their pristine and OH-adsorbed configurations (bottom panel). PDOS for both 0.25 ML Fe_{tet1} and 0.5 ML $Fe_{oct2-tet1}$ surface terminations are shown. The arrow marks indicate the formation of new bonding orbitals due to the interaction between the OH radical and the surface Fe atom. The energy is referenced to the Fermi-level.

dx.doi.org/10.1021/jp309434a | J. Phys. Chem. C 2013, 117, 5678−5683

PDOS plots of 0.25 and 0.5 ML cases, the new bonding states formed (indicated by black arrows) are around approximately −7 and −8 eV for the 0.25 and 0.5 ML cases, respectively. Thus, it can be observed that the energy gain produced by the orbital mixing, i.e. the energy difference between OH 3σ level and the corresponding new bonding states is greater for the 0.5 ML case.[27] This correlates well with a higher adsorption strength of −2.30 eV on the 0.5 ML $Fe_{oct2-tet1}$ surface compared to −1.11 eV on the 0.25 ML Fe_{tet1} surface.

Additionally, based on our Bader charge calculations, we estimated oxidation of the surface Fe atom relative to its bare state in both the cases. We found a charge transfer of 0.47 and 0.16 e to the O atom of the water molecule in the 0.5 and 0.25 ML cases, respectively, which enables the O atom to withdraw less charge from the H atom consequently loosening the O−H bond and favoring dissociation.

TMSR as a Surface Reactivity Descriptor. In order to build a descriptor to assess and compare the surface reactivity of Fe_3O_4 and $NiFe_2O_4$, we obtained the surface resonances (SRs) of the surface transition metal atom by calculating the difference between the surface and the bulk PDOS. SRs are positive peaks in the Fe DOS plot owing to the appearance of additional states at the surface relative to its bulk.[19] The center of gravity of the SRs (denoted as ε_{CCM}) is shown to be a good indicator of the surface reactivity for transition metal carbides.[19] The closer the ε_{CCM} is to the Fermi-level, the higher the reactivity.

Figure 6 shows the adsorption energy values of a dissociated water molecule as a function of the corresponding ε_{CCM} of the surface. We find a clear trend showing an increase in the adsorption energy as the ε_{CCM} is shifted toward the Fermi-level, indicating that transition metal SRs are good descriptors of the surface reactivity of the ferrites investigated here. Such descriptors are useful in tailoring the doping concentration of various transition metals in ferrite systems and subsequently designing efficient catalysts for multiple applications.

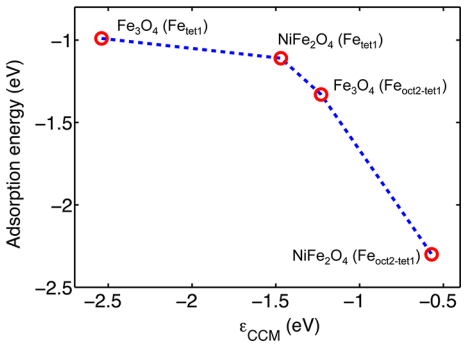

Figure 6. Variation of water adsorption energies with the descriptor ε_{CCM} (center of gravity of the TMSR).

CONCLUSIONS

In summary, we have shown that the reactivity of $NiFe_2O_4$ (111) surfaces is significantly higher compared to that of Fe_3O_4 (111) surfaces by assessing the energetics and kinetics of water adsorption and dissociation using the DFT + U approach. The surface structure of $NiFe_2O_4$ has been analyzed and both the 0.25 ML Fe_{tet1} and the 0.5 ML $Fe_{oct2-tet1}$ terminations are found to be stable under the possible range of oxygen chemical potential. The water adsorption energy values obtained for the $NiFe_2O_4$ case is much higher than the reported adsorption energy values for Fe_3O_4. We found a low activation barrier of 0.18 eV for single water molecule dissociation on the 0.25 ML Fe_{tet1} termination, while a barrierless dissociation on the 0.5 ML $Fe_{oct2-tet1}$ termination, which are of significance from the point of view of WGS reaction where water dissociation is an important factor controlling the efficiency. The surface reactivity is understood from the interaction of the OH molecular orbitals with the d states of the surface Fe atom. The new bonding orbitals created due to the interaction of the OH 3σ orbital and the Fe d states are pushed deeper down the energy axis resulting in a greater energy gain and higher water adsorption strength in the case of 0.5 ML $Fe_{oct2-tet1}$ termination. In addition, the reactivity is found to be correlated to the center of gravity of the SRs (ε_{CCM}) which could be a useful descriptor in a typical screening procedure for efficient ferrite-based catalysts. We believe that our findings have general implications in the field of catalysis and corrosion. In particular, we highlight the importance of $NiFe_2O_4$ as a catalyst in industrial reactions and the key role played by $NiFe_2O_4$ in fuel materials degradation in nuclear reactors.

ASSOCIATED CONTENT

Supporting Information

Additional details on the use of U = 3 eV; magnetization of Fe; structure files for the most stable adsorption configurations of water on $NiFe_2O_4$ (VASP structure file format). This material is available free of charge via the Internet at http://pubs.acs.org.

AUTHOR INFORMATION

Corresponding Author

*E-mail: byildiz@mit.edu; jcg@mit.edu.

Notes

The authors declare no competing financial interest.

ACKNOWLEDGMENTS

The authors acknowledge the financial support from the Consortium for Advanced Simulation of Light Water Reactors, an Energy Innovation Hub for Modeling and Simulation of Nuclear Reactors, under the U.S. Department of Energy Contract No. DE-AC05-00OR22725. P.V.K. thanks Jaguar for providing computational resources.

REFERENCES

(1) Henrich, V. E.; Cox, P. A. *The Surface Science of Metal Oxides*; Cambridge University Press: Cambridge, U.K., 1994.

(2) Rangel, M. d. C.; Sassaki, R. M.; Galembeck, F. Effect of Chromium on Magnetite Formation. *Catal. Lett.* **1995**, *33*, 237−254.

(3) Khan, A.; Chen, P.; Boolchand, P.; Smirniotis, P. G. Modified Nano-crystalline Ferrites for High-Temperature WGS Membrane Reactor Applications. *J. Catal.* **2008**, *253*, 91−104.

(4) Suzuki, Y. Epitaxial Spinel Ferrite Thin Films. *Annu. Rev. Mater. Res.* **2001**, *31*, 265−289.

(5) Reddy, G. K.; Gunasekera, K.; Boolchand, P.; Dong, J.; Smirniotis, P. G. High Temperature Water Gas Shift Reaction over Nanocrystalline Copper Codoped-Modified Ferrites. *J. Phys. Chem. C* **2011**, *115*, 7586−7595.

(6) Fritsch, D.; Ederer, C. Epitaxial Strain Effects in the Spinel Ferrites $CoFe_2O_4$ and $NiFe_2O_4$ from First Principles. *Phys. Rev. B* **2010**, *82*, 104117.

(7) Deshon, J.; Frattini, P. *Adsorption of Boric Acid on Synthetic Fuel Crud Oxides*; EPRI: Palo Alto, CA, 2002; p 1003384.

(8) Sawicki, J. A. Evidence of Ni_2FeBO_5 and m-ZrO_2 Precipitates in Fuel Rod Deposits in AOA-affected High Boiling Duty PWR Core. *J. Nucl. Mater.* **2008**, *374*, 248−269.
(9) Deshon, J. *PWR Axial Offset Anomaly (AOA) Guidelines, Revision 1*; EPRI: Palo Alto, CA, 2004; p 1008012.
(10) Kumar, P. V.; Short, M. P.; Yip, S.; Yildiz, B.; Grossman, J. C. First-Principles Assessment of the Reactions of Boric Acid on NiO(001) and ZrO2(−111) Surfaces. *J. Phys. Chem. C* **2012**, *116*, 10113−10119.
(11) Zhou, C.; Zhang, Q.; Chen, L.; Han, B.; Ni, G.; Wu, J.; Garg, D.; Cheng, H. Density Functional Theory Study of Water Dissociative Chemisorption on the Fe3O4(111) Surface. *J. Phys. Chem. C* **2010**, *114*, 21405−21410.
(12) Costa, A.; Lula, R.; Kiminami, R.; Gama, L.; de Jesus, A.; Andrade, H. Preparation of Nanostructured $NiFe_2O_4$ Catalysts by Combustion Reaction. *J. Mater. Sci.* **2006**, *41*, 4871−4875.
(13) Grillo, M. E.; Finnis, M. W.; Ranke, W. Surface Structure and Water Adsorption on Fe_3O_4(111): Spin-Density Functional Theory and On-site Coulomb Interactions. *Phys. Rev. B* **2008**, *77*, 075407.
(14) Rim, K. T.; Eom, D.; Chan, S.-W.; Flytzani-Stephanopoulos, M.; Flynn, G. W.; Wen, X.-D.; Batista, E. R. Scanning Tunneling Microscopy and Theoretical Study of Water Adsorption on Fe3O4: Implications for Catalysis. *J. Am. Chem. Soc.* **2012**, *134*, 18979−18985.
(15) Perron, H.; Mellier, T.; Domain, C.; Roques, J.; Simoni, E.; Drot, R.; Catalette, H. Structural Investigation and Electronic Properties of the Nickel Ferrite NiFe2O4: a Periodic Density Functional Theory Approach. *J. Phys.: Condens. Matter* **2007**, *19*, 346219.
(16) Fritsch, D.; Ederer, C. Effect of Epitaxial Strain on the Cation Distribution in Spinel Ferrites CoFe2O4 and NiFe2O4: a Density Functional Theory Study. *Appl. Phys. Lett.* **2011**, *99*, 081916.
(17) Cheng, Y.; Zheng, Y.; Wang, Y.; Bao, F.; Qin, Y. Synthesis and Magnetic Properties of Nickel Ferrite Nano-Octahedra. *J. Solid State Chem.* **2005**, *178*, 2394−2397.
(18) Son, S.; Taheri, M.; Carpenter, E.; Harris, V. G.; McHenry, M. E. Synthesis of Ferrite and Nickel Ferrite Nanoparticles Using Radio-Frequency Thermal Plasma Torch. *J. Appl. Phys.* **2002**, *91*, 7589−7591.
(19) Vojvodic, A.; Hellman, A.; Ruberto, C.; Lundqvist, B. I. From Electronic Structure to Catalytic Activity: A Single Descriptor for Adsorption and Reactivity on Transition-Metal Carbides. *Phys. Rev. Lett.* **2009**, *103*, 146103.
(20) Kresse, G.; Furthmüller, J. Efficient Iterative Schemes for Ab-initio Total-Energy Calculations Using a Plane-Wave Basis Set. *Phys. Rev. B* **1996**, *54*, 11169−11186.
(21) Blöchl, P. E. Projector Augmented-Wave Method. *Phys. Rev. B* **1994**, *50*, 17953−17979.
(22) Perdew, J. P.; Chevary, J. A.; Vosko, S. H.; Jackson, K. A.; Pederson, M. R.; Singh, D. J.; Fiolhais, C. Atoms, Molecules, Solids, and Surfaces: Applications of the Generalized Gradient Approximation for Exchange and Correlation. *Phys. Rev. B* **1992**, *46*, 6671−6687.
(23) Dudarev, S. L.; Botton, G. A.; Savrasov, S. Y.; Humphreys, C. J.; Sutton, A. P. Electron-Energy-Loss Spectra and the Structural Stability of Nickel Oxide: An LSDA+U Study. *Phys. Rev. B* **1998**, *57*, 1505−1509.
(24) Monkhorst, H. J.; Pack, J. D. Special Points for Brillouin-Zone Integrations. *Phys. Rev. B* **1976**, *13*, 5188−5192.
(25) Finnis, M. W.; Lozovoi, A. Y.; Alavi, A. The Oxidation of NiAl: What Can We Learn from Ab Initio Calculations? *Annu. Rev. Mater. Sci.* **2005**, *35*, 167−207.
(26) Zhang, J.; Shi, J.; Gong, M. Synthesis of Magnetic Nickel Spinel Ferrite Nanospheres by a Reverse Emulsion-assisted Hydrothermal Process. *J. Solid State Chem.* **2009**, *182*, 2135−2140.
(27) Carrasco, J.; Michaelides, A.; Scheffler, M. Insight from First Principles into the Nature of the Bonding between Water Molecules and 4d Metal Surfaces. *J. Chem. Phys.* **2009**, *130*, 184707.